Acta Oceanol. Sin., 2024, Vol. 43, No. 11, P. 88–98
https://doi.org/10.1007/s13131-024-2381-0
http://www.aosocean.com
E-mail: ocean2@hyxb.org.cn

Dynamic of phytoplankton community during varying intensities of the northeast monsoon in the Taiwan Strait

Yanping Zhong[1, 2], Peixuan Wang[1], Jinxin Chen[1], Xin Liu[1, 3*], Edward A. Laws[4], Bangqin Huang[1, 3]

[1] National Observation and Research Station for the Taiwan Strait Marine Ecosystem/Fujian Provincial Key Laboratory of Coastal Ecology and Environmental Studies, College of the Environment and Ecology, Xiamen University, Xiamen 361102, China

[2] Fujian Province Key Laboratory for the Development of Bioactive Material from Marine Algae, College of Resources and Environmental Sciences, Quanzhou Normal University, Quanzhou 362000, China

[3] Southern Marine Science and Engineering Guangdong Laboratory (Zhuhai), Zhuhai 511458, China

[4] Department of Environmental Sciences, College of the Coast & Environment, Louisiana State University, Baton Rouge 70803, LA, USA

Received 15 March 2024; accepted 7 May 2024

Abstract

The characteristics of the terrain of a strait can lead to a "fine tube" effect that enhances a monsoon and thereby affects the physical, chemical, and biological processes of marine ecosystems. This effect is a highly dynamic and complex phenomenon involving interactions among atmospheric, oceanic, and terrestrial systems, as well as biogeochemical cycles and biological responses driven by it. However, current understanding has been focused mainly on the differences between monsoons, and there have been few studies concerned with the weakening or strengthening of monsoons. To explore the biogeochemical and phytoplankton responses during varying intensities of the northeast (NE) monsoon in the Taiwan Strait, high-resolution, across-front observations combined with FerryBox online data and satellite observations were conducted in this study during a strong, moderate, and weak NE monsoon. The spatiotemporal changes of nutrient concentrations and phytoplankton communities were regulated by the dynamics of ocean currents forced by NE winds. The weakening of the NE monsoon caused shrinkage of the coastal currents that led to a reduction of nutrient concentrations and an alteration of the distribution patterns of phytoplankton communities along cross-front sections. Specifically, there was a notable decrease in the proportions of dinoflagellates and cryptophytes in inshore regions and of prasinophytes in offshore areas. This study showed for the first time the dynamics of phytoplankton with changes of ocean currents during varying intensities of the NE monsoon in a strait system. The findings helped to elucidate the general spatial patterns of the phytoplankton community based on satellite-derived surface temperature and wind patterns and further enhanced the understanding of biogeochemical cycles in marine systems.

Key words: monsoon, coastal current, front, phytoplankton community, Taiwan Strait

Citation: Zhong Yanping, Wang Peixuan, Chen Jinxin, Liu Xin, Laws Edward A., Huang Bangqin. 2024. Dynamic of phytoplankton community during varying intensities of the northeast monsoon in the Taiwan Strait. Acta Oceanologica Sinica, 43(11): 88–98, doi: 10.1007/s13131-024-2381-0

1 Introduction

Marine phytoplankton are influenced by a variety of environmental factors that are strongly associated with monsoonal, wind-driven forcing, especially in the region of the East Asia monsoon. These monsoonal dynamics significantly influence the degree of mixing of the water column and thereby affect the availability of nutrients, which in turn influences phytoplankton biomass and composition. For example, in the South China Sea (SCS) basin, lower chlorophyll *a* (Chl *a*) concentrations have been observed during the weak southwest (SW) monsoon, when there is shoaling of the mixed layer depth, whereas higher Chl *a* concentrations have been observed during the strong northeast (NE) monsoon, because the enhanced mixing pumps additional nutrients into the euphotic zone (Yu et al., 2019). Furthermore, monsoons can influence mesoscale physical processes, such as the intensities of intrusions of coastal currents, and thus affect the function of marine systems (Parab et al., 2006; Lai et al., 2021).

Variations of the intensity of a monsoon cause changes of ocean circulation, which further affect the hydro-physical, chemical, and biological processes of marine ecosystems because different currents transport specific water masses that have characteristic temperatures, salinities, and nutrient concentrations (Belkin et al., 2009). These characteristics lead to the formation of some unique phytoplankton groups in the current systems. For instance, in the New Guinea Coastal Current, diatoms and dinoflagellates are relatively abundant, whereas cyanobacteria are dominant in the Northern Equatorial Counter Current (Mascioni et al., 2023). Furthermore, variations of ocean currents control the spatial dynamics of particular species and thus influence the composition of the phytoplankton. This influence was evidenced by the effect of the North Atlantic Current, which expands the

Foundation item: The National Natural Science Foundation of China under contract Nos 42122044, 42206100, and 42141002; the Found of Southern Marine Science and Engineering Guangdong Laboratory (Zhuhai) under contract No. SML2021SP308.
*Corresponding author, E-mail: liuxin1983@xmu.edu.cn

spatial distribution of the coccolithophore *Emiliania huxleyi*, a temperate phytoplankton, in the Arctic Ocean (Oziel et al., 2020). Therefore, the dynamic of phytoplankton community was linked with the variations of ocean circulations, and exploring the response of the phytoplankton community to the monsoon-induced ocean current dynamics can deepen understanding of the ecological responses of marine systems.

In a strait system, the "narrow tube" effect is enhanced under the combined effects of a narrow channel and strong monsoon (Chen and Lin, 2022). This combination facilitates observing the ecological responses of marine systems to monsoon-driven variations of ocean currents. The Taiwan Strait (TWS) is an important channel about 350 km long that separates the East China Sea and SCS (Hong et al., 2011a), and its circulation is regulated by the East Asia monsoon. Our previous studies have shown that monsoonal winds are the dominant factors that regulates mesoscale physical processes, including the intrusion of the coastal current during the NE monsoon (Zhong et al., 2020) and upwelling during the SW monsoon (Zhong et al., 2019), and then influence the distribution patterns of phytoplankton biomass and community (Zhong et al., 2020). During the SW monsoon, strong upwelling driven by prevailing SW winds increased the concentrations of total chlorophyll *a* (TChl *a*)and diatoms within coastal zones. In contrast, stratification over the continental shelf that restricted the upward transport of nutrients resulted in reduced phytoplankton biomass (Zhong et al., 2020). During the NE monsoon, the Zhe-Min Coastal Current (ZMCC), which is characterized by low temperature and low salinity, moves from northeast to southwest, and the warmer and higher-salinity current formed by the Kuroshio branch water and the subsurface water of the SCS flows northward into the central TWS (Kuo and Ho, 2004; Hu et al., 2010). The coastal currents with relatively low temperature and high nutrient concentrations and intense vertical mixing driven by prevailing NE winds elevated TChl *a* concentrations and play a vital role in supporting the growth of phytoplankton groups, including dinoflagellates, cryptophytes, and diatoms in the coastal waters of the TWS (Zhong et al., 2020). They explain then the tight coupling between TChl *a* concentrations and coastal currents in the TWS during the NE monsoon (Hong et al., 2011b). Meanwhile, the convergence of distinct water masses frequently results in the formation of thermal or salinity fronts in the TWS, and the high abundance of fish in the frontal zone along the Zhe-Min coast, evidenced by the Zhoushan fishery, has been well documented (He et al., 2016). The position, bread, and intensity of the thermal fronts showed seasonal variations (He et al., 2016), which is tightly coupled with the speed of the NE monsoon wind (Zhang et al., 2020). Several studies have focused that the dynamic of phytoplankton biomass and community in the frontal zones (Flint et al., 2002; Taylor et al., 2012; Clayton et al., 2014). For instance, Taylor et al. (2012) have found that phytoplankton biomass at the frontal zones significantly increased compared to the surrounding waters, and phytoplankton were dominated by large-sized diatoms. While, the understanding of dynamic of phytoplankton biomass and communities across the frontal zones formed by the convergence of the costal current and warm current was lacking. Exploring the ecological responses to variations of the NE monsoon-driven ocean current would thus be pivotal for elucidating the biogeochemical cycles in the TWS.

Current understanding focused on the TWS is the general variation patterns of the monsoon climate state, but there are highly dynamic spatiotemporal changes and complex physical, chemical and biological coupling processes behind it. In the TWS, a strong NE monsoon typically prevails from October to March and begins to decline in April. May is a transitional period (Hong et al., 2011a) (Fig. 1). Several studies have shown that phytoplankton biomass in the TWS varied with the intensity of the NE monsoon wind (Shang et al., 2005; Zhao et al., 2022), and dynamics of physical, chemical, and biological processes with the varying intensities of the NE monsoon have remained unclear. Focusing on the coupling between dynamic physical drivers and complex biological responses of the monsoon requires field observations to obtain higher resolution and multidisciplinary synchronized results, which were difficult to achieve in the past. In this study, we conducted three cruises with high-resolution observations and FerryBox data across temperature fronts in the central TWS during March, April, and May to clarify the biological responses to the variations of ocean currents during different intensities of the NE monsoon. We expected that our findings would deepen understanding of the responses of multiple processes in the TWS during the NE monsoon and the impact of those changes on fisheries and the biogeochemical cycles.

2 Materials and methods

2.1 *Study areas and sampling*

To explore the responses of phytoplankton in the TWS to changes of ocean currents with different intensities of the NE monsoon, we conducted across-front cruises in the TWS onboard the R/V *Yanping 2*. We captured three NE monsoonal intensities in the TWS bounded by latitudes of 20°N and 27°N and longitudes of 115°E and 122°E : a weak phase from May 14 to 20, 2017 with mean wind speed of 1.8 m/s before two weeks of the observations, a moderate phase from April 21 to 22, 2018 with mean wind speed of 3.9 m/s before two weeks of the observations, and a strong phase from March 18 to 19, 2019 with mean wind speed of 5.1 m/s before two weeks of the observations (Fig. 2). The cross-front transects— A and B in May 2017, E and F in April 2018, and G and H in March 2019—involved sampling from the nearshore to offshore areas. We collected samples along all the transects, but detailed analyses of physical, chemical, and biological parameters were made on Transect G in 2019, Transect E in 2018, and Transect A in 2017. These transects corresponded to strong, moderate, and weak NE winds, respectively. The physical, chemical, and biological conditions along Transects H, E, B were similar with those along Transects G, F, and A, respectively. Stations H5, H6, E12, and B9 were located at the temperature frontal zone (Figs S1–S5). Information of the physical, chemical, and biological parameters about the three sections is provided in the attachment (Figs S2–S4).

2.2 *Measurements of physicochemical and biological parameters*

Surface values of temperature, salinity, and Chl *a* fluorescence were taken from FerryBox data. Vertical profiles of temperature and salinity were directly recorded, and water samples were collected with a conductivity-temperature-depth (CTD) system (Seabird SEB 19). The mixed layer depth (MLD) was defined as the depth at which the seawater density exceeded that at 5 m by 0.125 kg/m^3 (Thomson and Fine, 2003). Nutrient samples were measured with a QUAATRO nutrient analyzer. The detection limits of nitrate + nitrite (NO_X), phosphate, and silicate were 0.03 μmol/L, 0.02 μmol/L, and 0.1 μmol/L, respectively (Zhong et al., 2022).

Seawater of 1–4 L was filtered through 25 mm GF/F filters (Whatman) and the filters stored in liquid nitrogen for analysis of phytoplankton photosynthetic pigments. In the laboratory, the filters were kept at –80℃, and then pigment concentrations were

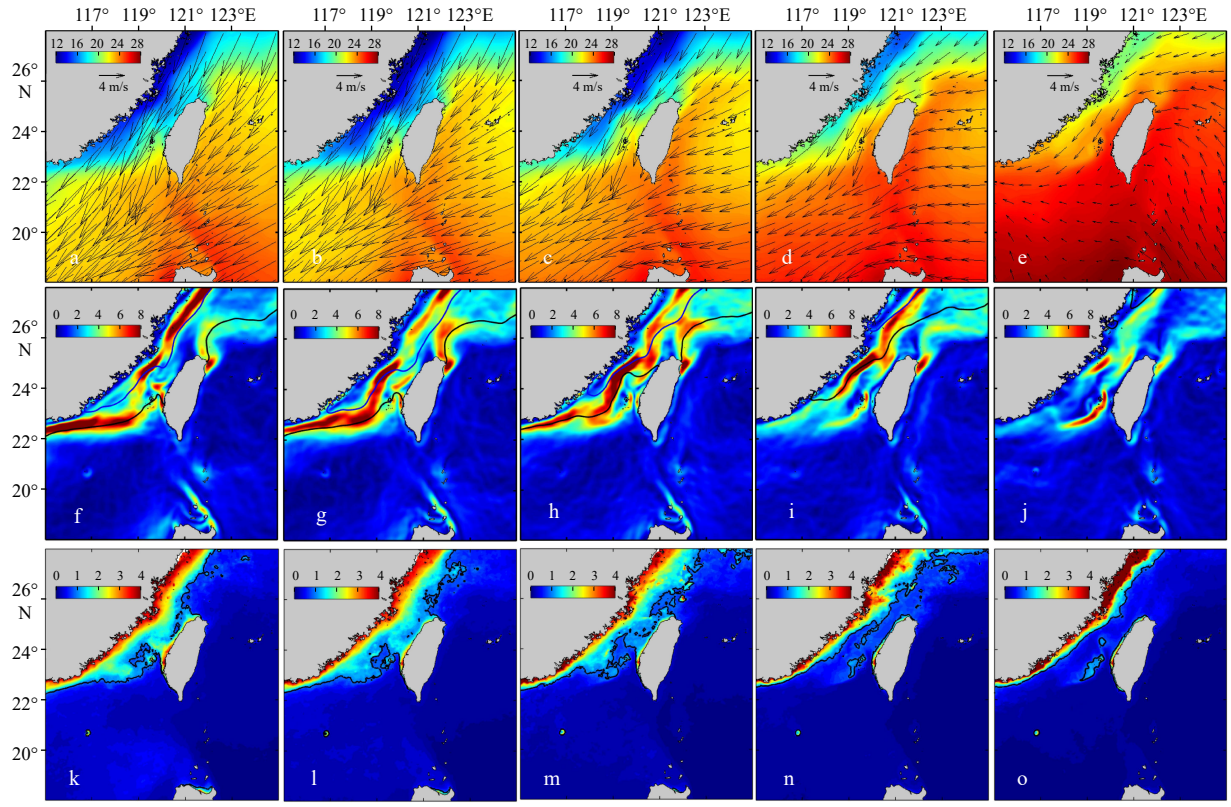

Fig. 1. The mean sea surface temperature (℃, a–e), wind velocity at 10 m above the sea surface (vectors, m/s, a–e), the horizontal gradient of temperature [℃/(100 km), f–j] and chlorophyll *a* concentration (μg/L, k–o) in the Taiwan Strait in January (a, f, k), February (b, g, l), March (c, h, m), April (d, i, n), May (e, j, o) between 2010 and 2022. The blue and black lines represent the 17℃ and 20℃ isotherms.

assessed using high-performance liquid chromatography (HPLC) following the combination of equal volumes of ammonium acetate and the extract solution obtained from filters treated with N, N-dimethylformamide. Phytoplankton groups, including dinoflagellates, diatoms, haptophytes Type 8, haptophytes Type 6, chlorophytes, cryptophytes, *Prochlorococcus*, *Synechococcus*, and prasinophytes, were determined according to the methods described by Zhong et al. (2020). Some hydrological parameters and nutrient concentrations during the cruise in March 2019 have been published in Zhao et al. (2022) to document the phytoplankton bloom off the coast in the TWS during the time of relaxation of the northeasterly monsoon.

2.3 *Satellite data*

Daily sea surface temperature (SST) with a spatial resolution of 0.05° and monthly mean Chl *a* concentrations with a resolution of 4 km were derived from the Copernicus Marine Environment Monitoring Service (available at https://resources.marine.copernicus.eu/product-download/SST_GLO_SST_L4_REP_OBSERVATIONS_010_011) and the Moderate Resolution Imaging Spectroradiometer (MODIS) database from January 2010 to December 2022 (available at https://oceancolor.gsfc.nasa.gov/), respectively. The identification of temperature fronts based on the gradient analyses were determined using the methods of Belkin et al. (2009). Based on satellite-derived data between 2010 to 2022, we calculated the climatological averages of SST, temperature gradients, and Chl *a* in the surface water of the TWS between January and May. The eastward and northward components of daily and monthly mean wind velocity were obtained from the Cross-calibrated Multi-Platform database (available at https://data.remss.com/ccmp/v03.1/) and were used to calculate the mean wind speed two weeks before the observations and climatological averages of wind speed between January and May.

2.4 *Statistical analyses*

All statistical analyses were done using R software version 3.6.3 (R Core Team, 2020). The "Vegan" package in R was used to carry out the principal coordinates analysis (PCoA) and canonical correspondence analysis (CCA). PCoA and CCA were used to explain how the dynamics of the phytoplankton community in the TWS were related to the variations of ocean currents that were regulated by the NE monsoon. PCoA was used to discern the differences between phytoplankton communities in different regions, including the coastal areas, frontal zones, and offshore areas based on the surface dataset from all transects during the three cruises. CCA was conducted to explore the effect of environment factors on the phytoplankton communities based on the combined dataset of the three cruises. Figs 2–4 and S4–S5 were plotted with Ocean Data View software (Schlitzer, 2020).

3 Results

3.1 *Variations in physical parameters with different intensities of the NE monsoon*

The speed of the NE winds progressively declined from January to May (Fig. 1). These winds strongly influenced the SST of the coastal current, which was lowest (<17℃) in January and February. The NE winds then decreased markedly from March to May. The fact that changes of the SST gradients and Chl *a* concentrations paralleled trends of SST suggested that variations of

the observed physical and biological processes from March to May were associated with the dynamics of the coastal current, which was modulated by the NE wind.

The satellite database revealed distinctly different wind fields and patterns of SST distributions during the three cruises with different intensities of NE monsoon. The areas of low temperature (<17℃) were the most extensive during the observations in 2019 with strong NE wind (followed by the moderate wind), and we found an obvious temperature front with temperature gradients of exceeding 8℃/km in the central TWS. The time of the weak NE wind during the observations in 2017 was characterized by the smallest area of low temperature and the absence of a temperature front most of the time (Figs 2a–f).

A difference of physical properties on vertical profiles was apparent during varying intensities of the NE wind (Figs 3 and 4). During the observation in March 2019 with the strong NE wind, nearshore stations of the cross-front were impacted by the coastal current, which was characterized by low temperatures (<17℃) and low salinity (<31), while offshore stations were characterized by warm currents with higher temperatures (>22℃) and higher salinity (>34) and were a mixture of the SCS and Kuroshio waters (Fig. 3). There was a significant upward doming of isopycnals near the offshore distance of 55 km (near 119.6°E), where intense stratification above 10 m was apparent (Fig. 3) along Transect G. This stratification aligned with the areas of abrupt changes of temperature and salinity based on FerryBox underway observations (Fig. 2g). Rapid transitions of temperature and salinity (from 16.81℃ to 22.92℃ and 31.40 to 34.45, respectively) were observed from 119.54°E to 119.60°E (Fig. 2g). Consequently, Stations G11, G12, G13, and G14 were located in the zone of temperature fronts.

Distributions of temperature and salinity along Transect F during the observation of April 2018 with moderate NE winds were similar to those during strong NE winds periods, but the overall temperature increased significantly during the former (Figs 3 and 4). The water in the cross-front section was characterized by a mixture of coastal water and SCS water (Fig. 3). There was an upward doming of isopycnals near the offshore distance of 60 km (near 119.95°E) (Fig. 4h), with swift changes in physical parameters at Station F3, which we designated as the temperat-

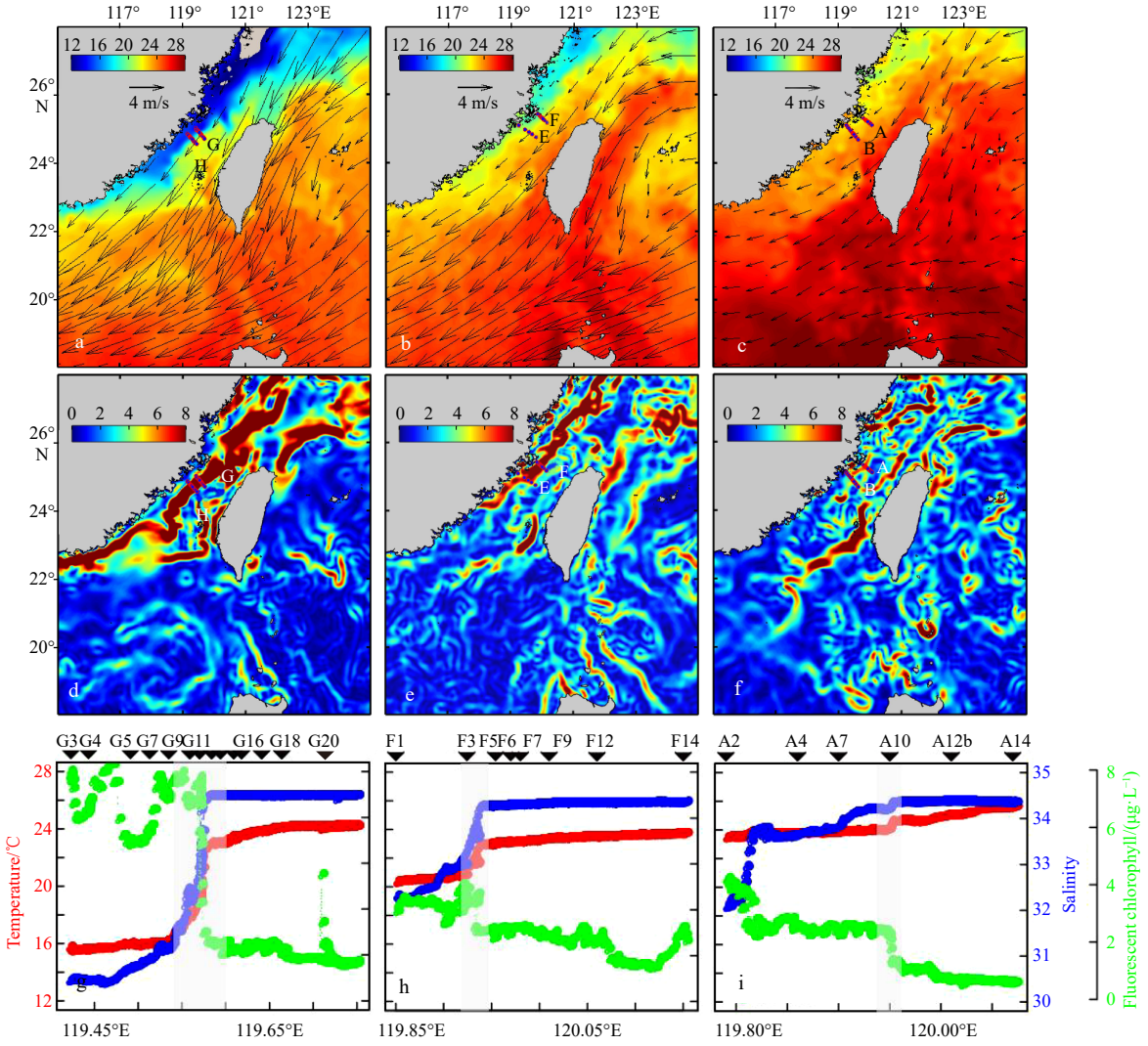

Fig. 2. Averaged SST (shading, ℃) during the observations in March 2019 (a), April 2018 (b), and May 2017 (c); and averaged wind velocity at 10 m above the sea surface (vectors, m/s, a–c) in the Taiwan Strait before two weeks of the observations in March 2019 (a), April 2018 (b), and May 2017 (c). The horizontal gradient of temperature [℃/(100 km)] in the Taiwan Strait during observations with strong (d), moderate (e), and weak (f) NE wind; changes of temperature, salinity, and fluorescent chlorophyll along Transects G, F, and A during the cruises of 2019 (g), 2018 (h) and 2017 (i). The grey rectangles represent the frontal zones.

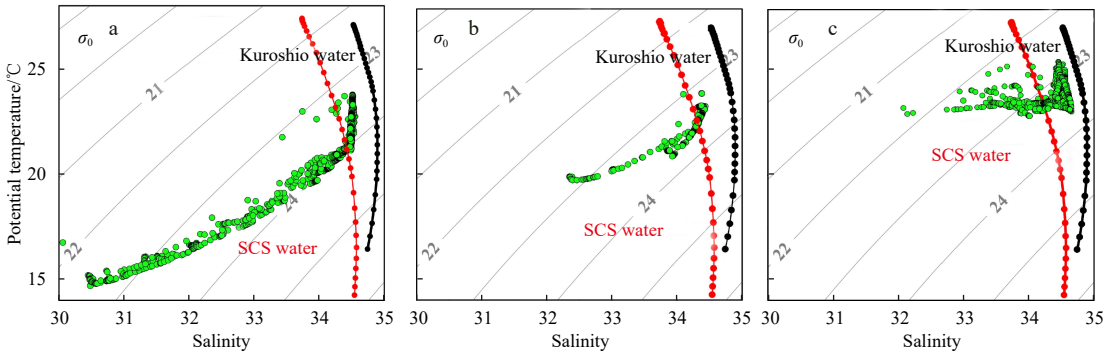

Fig. 3. Potential temperature–salinity diagrams during the observations with the strong (a), moderate (b), and weak (c) NE wind.

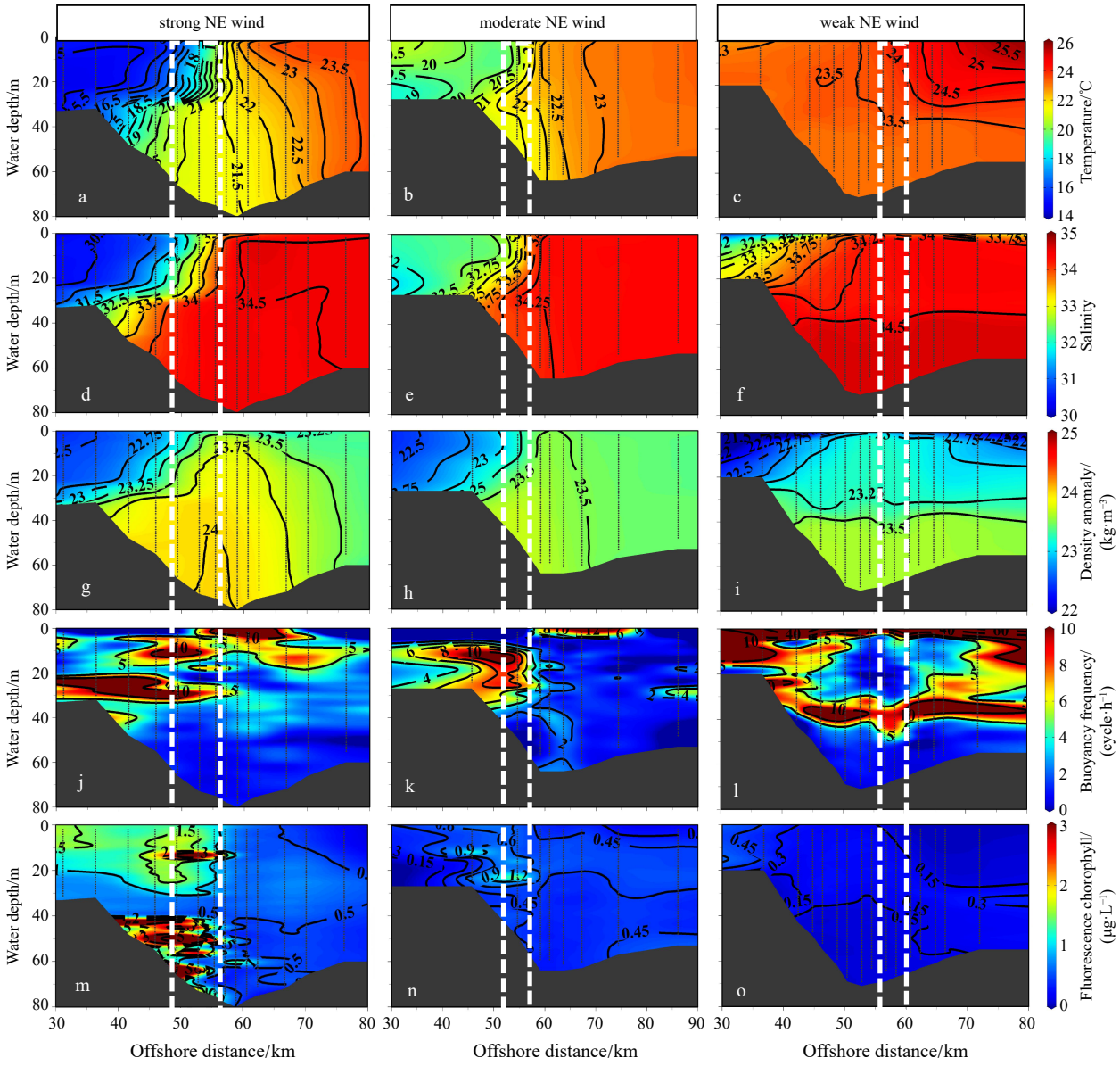

Fig. 4. Vertical profiles of sea temperature (℃, a, b, c), salinity (d, e, f), potential density anomaly (kg/m³, g, h, i), buoyancy frequency (cycle/h, j, k, l), and fluorescence chorophyll (μg/L, m, n, o) along Transects G (a, d, g, j, m), F (b, e, h, k, n), and A (c, f, i, l, o) under the forcing of strong, moderate, and weak NE wind. Stations in white frames represent the frontal zones.

ure frontal zone. The surface temperature and salinity recorded by the FerryBox system shifted from 20.61℃ to 22.82℃ and 32.87 to 34.22, respectively (Fig. 2h).

In contrast, the period of weak NE winds in May 2017 differed from the other periods. Excluding the surface layer (3 m), which was impacted by diluted water, the nearshore of the cross-front

transect was minimally affected by the coastal current along Transect A. The offshore was predominantly occupied by high-temperature and high-salinity waters (T > 23℃ and S > 34; Fig. 3c). Highly-salinity waters (S > 34.5) were located below 40 m. The slight change of the surface temperature along Transect A near 119.95°E indicated that Station A10 was located within the frontal zone (Fig. 4).

3.2 *Variations in chemical parameters with different intensities of the NE monsoon*

During the period of March 2019 with the strong NE monsoon, the distribution of currents closely reflected that of nutrient concentrations along Transect G (Figs 5a, d and g). The nutrient concentrations were elevated at nearshore stations, and concentrations of NO_X ranged from 0.62 μmol/L to 20.55 μmol/L, phosphate from 0.3 μmol/L to 0.9 μmol/L, and silicate from 2.11 μmol/L to 24.86 μmol/L. At offshore stations, vertical profiles of nutrients were homogeneous. The NO_X, phosphate, and silicate concentrations were below 4 μmol/L, 0.05 μmol/L, and 4 μmol/L, respectively (Figs 5a, d and g). The distribution patterns of nutrient concentrations were similar during the periods of moderate and strong NE monsoons, but nutrient concentrations were significantly lower during the former (Figs 5b, e and h). As the NE monsoon weakened, nutrient concentrations decreased further during the weak NE monsoon (Figs 5c, f and i).

3.3 *Distribution patterns of phytoplankton communities during different intensities of the NE monsoon and its influencing factors*

There were significant spatiotemporal variations of phytoplankton biomass and community composition across the front (tested by ANOSIM, p < 0.001). The fluorescent chlorophyll signal based on the FerryBox underway system and TChl *a* based on HPLC both declined rapidly within the frontal zones across three periods, especially during the observation of 2019 with strong NE winds (Figs 2, 2h, 2i, 6, 7 and S1). The TChl *a* concentrations in the nearshore surface waters of the temperature frontal zones were high. The average concentrations were 1.49 μg/L and 0.65 μg/L during observations of 2019 with strong NE wind and 2017 with weak NE wind, respectively (Figs 6a and c). Conversely, the TChl *a* concentrations on the opposite side of the front were low. They averaged 0.51 μg/L and 0.19 μg/L during periods of strong and weak NE monsoons, respectively (Figs 6a and c). During the observation of April 2018 with the moderate NE monsoon, the TChl *a* concentrations decreased at the frontal zone and underwent small variations along the cross-front sections (Figs 7 and S4–S5).

During the observation of 2019 with the strong NE monsoon, diatoms dominated the phytoplankton community. They contributed 17.1%–54.9% of the surface TChl *a* and 21.2%–64.7% of the depth-integrated average TChl *a*. The abundance of diatoms decreased from the nearshore to offshore areas (Figs 6 and 7). The concentrations of dinoflagellates and cryptophytes decreased in a similar manner. In contrast, the proportions of haptophytes Type 8, *Prochlorococcus*, *Synechococcus*, and prasinophytes increased from the nearshore to offshore areas (Figs 6 and 7). During the observation of April 2018 with the moderate NE monsoons, diatoms remained dominant and varied only slightly along the cross-front transect (Figs 6 and 7). During the observation of May 2017 with weak NE monsoons, proportions of diatoms, cryptophytes, and dinoflagellates obviously decreased, whereas groups such as haptophytes Type 8, *Prochlorococcus*, and *Synechococcus* increased in the offshore areas (Fig. 6).

The PCoA analysis clearly differentiated three groups (tested by ANOSIM, p < 0.001). Phytoplankton communities associated with the coastal current during the periods of strong NE winds in

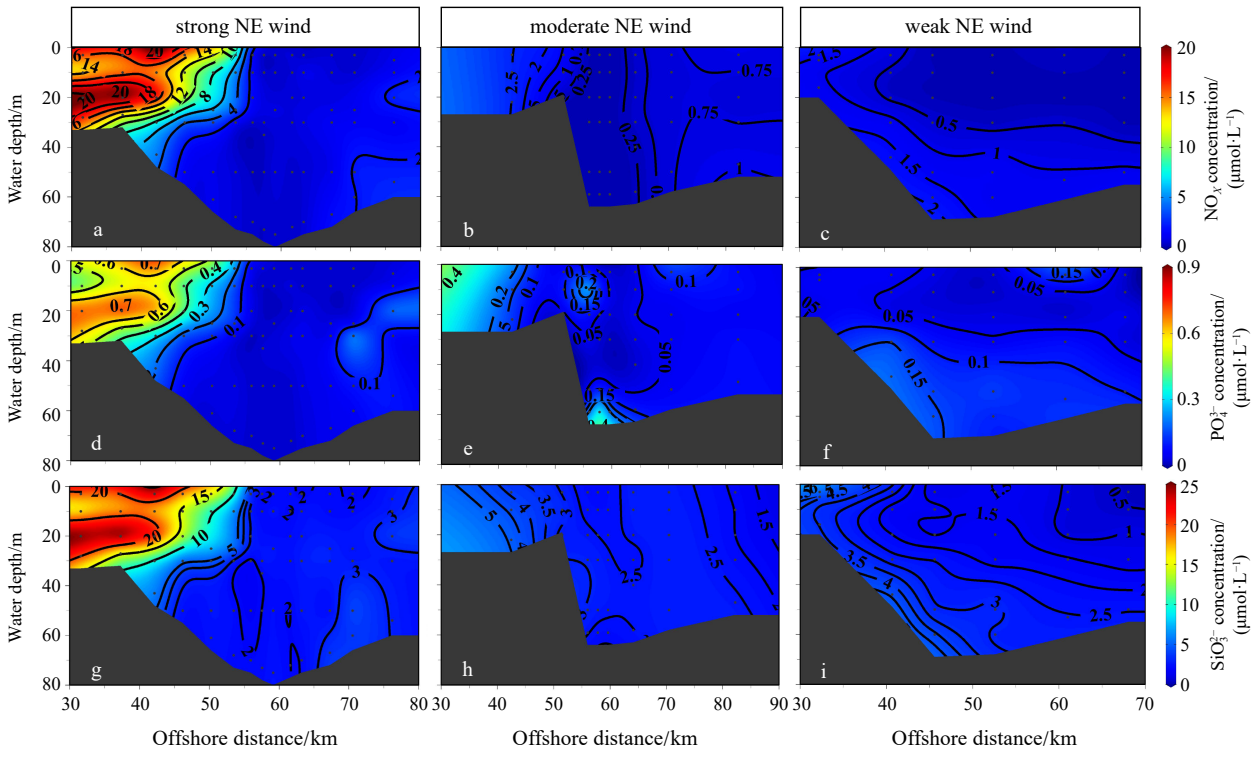

Fig. 5. Vertical profiles of nitrate + nitrite (NO_X, μmol/L, a, b, c), phosphate (PO_4^{3-}, μmol/L, d, e, f), and silicate (SiO_3^{2-}, μmol/L, g, h, i) along the Transects G (a, d, g), F (b, e, h), and A (c, f, i) under the forcing of strong, moderate, and weak NE wind.

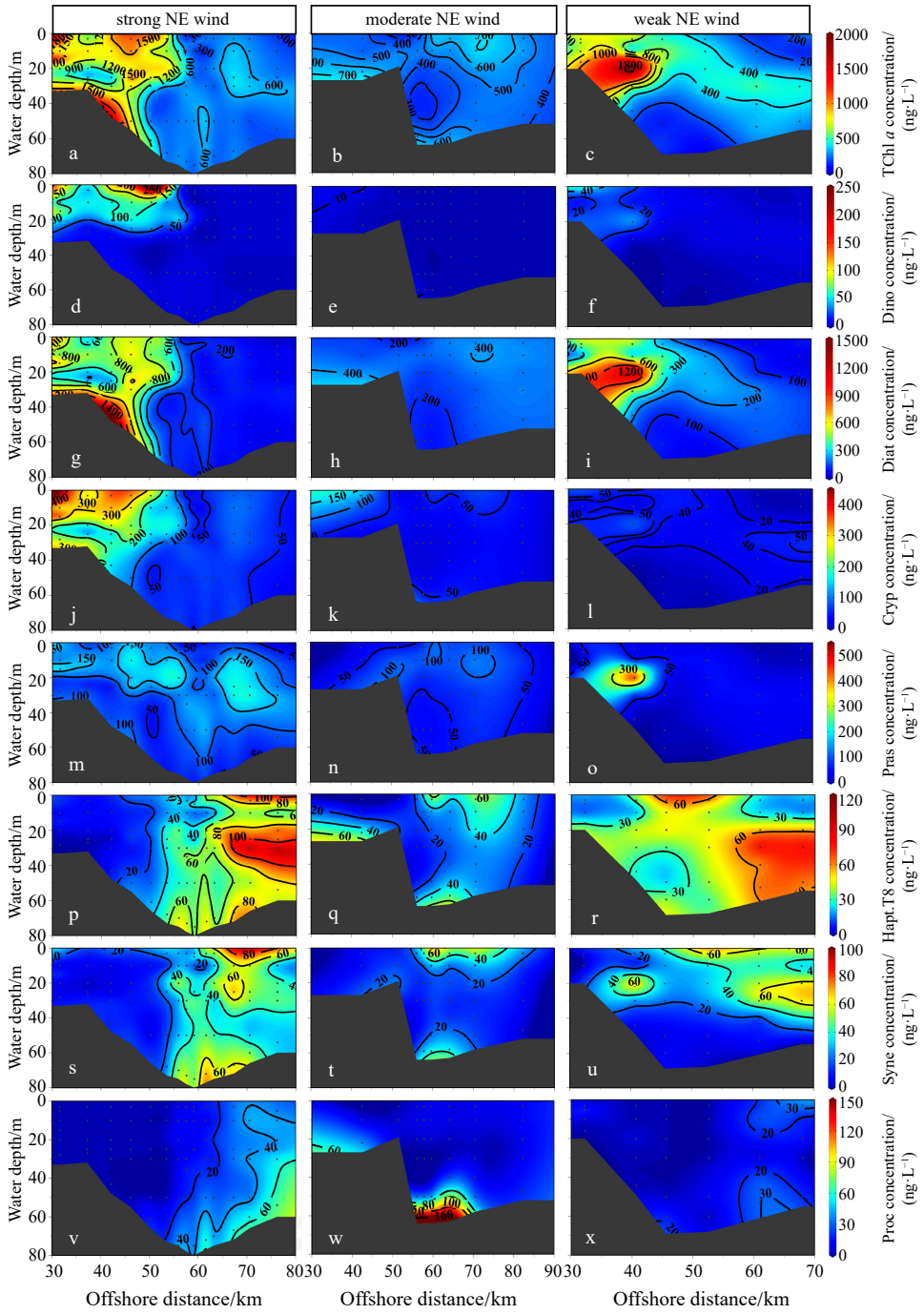

Fig. 6. Vertical profiles of total chlorophyll *a* (TChl *a*)(ng/L, a, b, c), dinoflagellate (Dino, ng/L, d, e, f), diatoms (Diat, ng/L, g, h, i), cryptophytes (Cryp, ng/L, j, k, l), prasinophytes (Pras, ng/L, m, n, o), haptophytes Type 8 (Hapt. T8, ng/L, p, q, r), *Synechococcus* (Syne, ng/L, s, t, u), and *Prochlorococcus* (Proc, ng/L, v, w, x) concentrations along the Transects G (a, d, g, j, m, p, s, v), F (b, e, h, k, n, g, t, w), and A (c, f, i, l, o, r, u, x) under the forcing of strong, moderate, and weak NE wind.

March 2019 were situated on the negative end of the first PCoA axis (Fig. 8). In contrast, communities influenced by the warm current during the periods of weak NE winds in May 2017 were on the positive end, and communities during the observation of April 2018 with the moderate NE winds occupied an intermediate position (Fig. 8a). According to the CCA analysis, environmental metrics explained 50.4% of the variances of the phytoplankton community during the three cruises. The close correlations between environmental variables, including nutrients and TChl *a*, and wind speed indicated that the increase of the concentration of nutrients carried by the coastal currents with increasing wind speed stimulated the growth of phytoplankton. Phytoplankton groups, including diatoms, dinoflagellates, chlorophytes, prasinophytes, and cryptophytes, were located on the positive side of the first CCA axis, close to the nutrient concentrations and wind speed, and far from temperature and salinity. Among the phytoplankton, dinoflagellates and cryptophytes were significantly correlated with NO_X and wind speed. The fact that other groups, including *Synechococcus*, *Prochlorococcus*, and haptophytes, were aligned closely with temperature and salinity

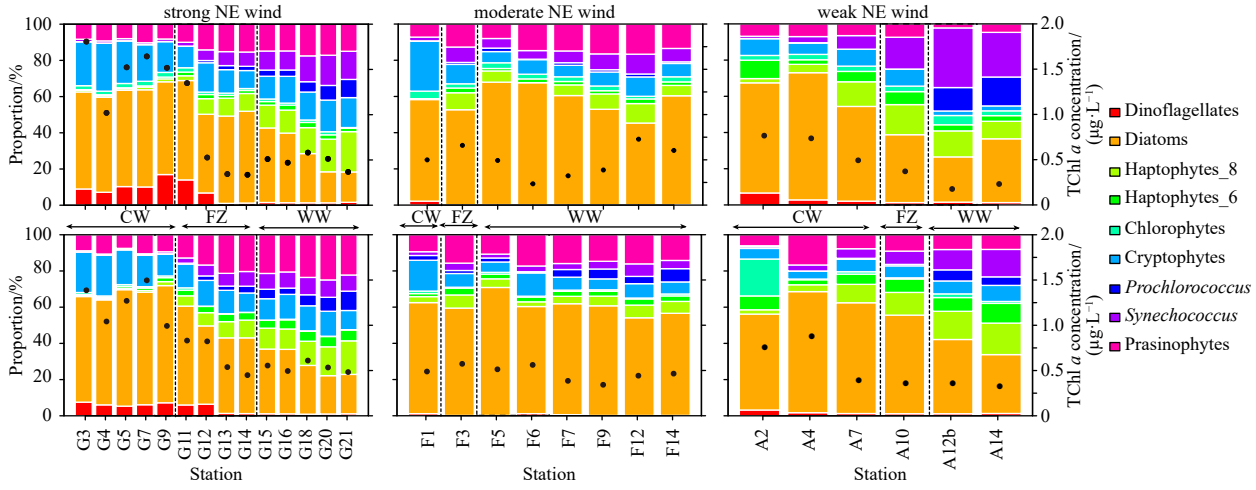

Fig. 7. Phytoplankton compositions in the surface water (upper) and average depth-integrated (bottom) along Transects G (left), F (middle), A (left) under the forcing of strong, moderate, and weak NE wind. CW: coastal water; FZ: frontal zone; WW: warm water.

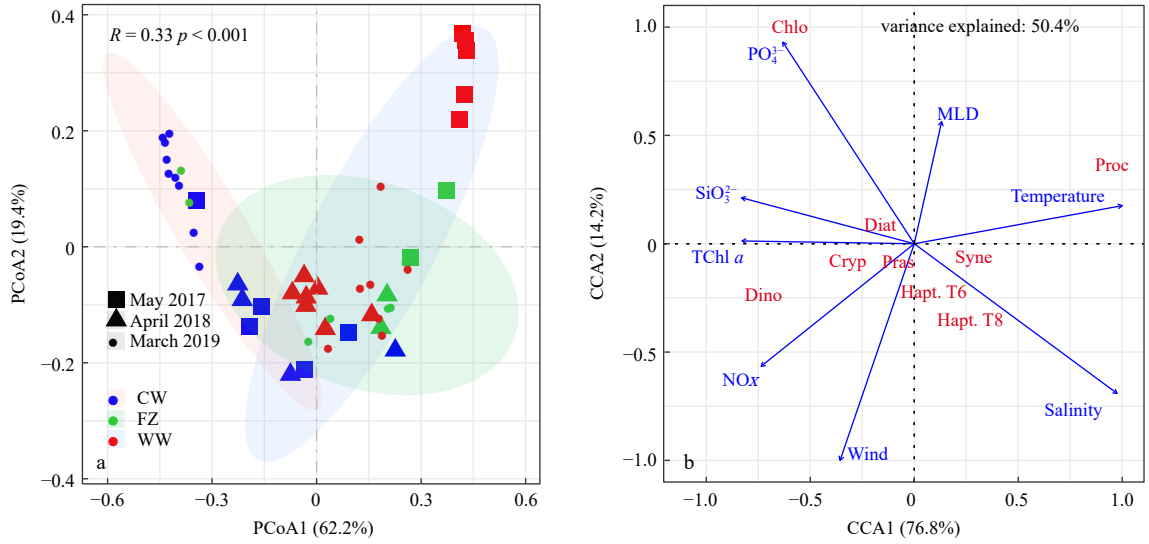

Fig. 8. Principal coordinates analysis (PCoA) based on the Bray-Curitis dissimilarities of the phytoplankton community in different zones (a), and canonical correlation analysis (CCA) of phytoplankton community and environmental factors (b). CW: coastal water; FZ: frontal zone; WW: warm water.

indicated an affinity for conditions prevalent within warm, current-influenced environments (Fig. 8b).

4 Discussion

4.1 *Association of phytoplankton community variations with the monsoon cycle*

The TWS comes under the influence of the East Asia monsoon system, and the stratification in the water column and mesoscale physical processes such as upwelling and the intrusion of coastal currents are influenced by the wind patterns (Hong et al., 2011a). Our previous studies have established a robust link between the seasonal dynamics of phytoplankton biomass and community composition in the TWS and monsoonal, wind-driven forcing during the NE and SW monsoons (Hong et al., 2011b; Zhong et al., 2020). Similar findings have been reported in many regions such as the Arabian Sea (Parab et al., 2006), the SCS (Yu et al., 2019), and the Kuroshio Current off the East Coast of Taiwan (Lai et al., 2021). These further suggest that there is a significant influence of seasonal cycles of the monsoon on the distribution patterns of phytoplankton biomass and compositions. However, the current understanding of monsoon-driven marine systems, such as in the TWS and Arabian Sea, has predominantly emphasized the differences between the NE and SW monsoons. There has been limited exploration of ecological responses in the marine systems during the transition of monsoon, due to the lack of filed observations under challenging sea conditions. Consequently, based on previous studies, this study further focused on the physical, chemical and biological processes under the varying intensities of NE monsoon. The influence of the coastal current was closely related to the speed of the NE monsoon (Zhang et al., 2020). This relationship was consistent with results based on decadal-scale satellite data, which have shown that the coastal currents change significantly in response to the NE winds from January to May (Fig. 1). The implication is that dynamics of the physical, chemical, and biological processes

in the TWS are strongly linked with the variations of the coastal currents forced by the speed of the NE monsoon wind. Therefore, clarifying the dynamics of phytoplankton biomass and communities during the varying intensities of NE monsoon help to understand the biogeochemical cycles in the TWS.

4.2 *Dynamics of phytoplankton biomass and community during varying intensities of NE monsoon*

The results during varying intensities of the NE monsoon suggested that variations of phytoplankton biomass and community composition were associated with mesoscale circulation dynamics driven by NE wind. When the NE wind was strong, the influence of the coastal current was enhanced within coastal regions, and the transport of nutrients accelerated the growth of specific phytoplankton groups such as diatoms, dinoflagellates, and cryptophytes (Figs 6, 7 and S4, S5). These groups abundances were positively correlated with nutrient concentrations and wind speeds, and their niches were characterized by low temperature, low salinity, and relatively high nutrient concentrations (Zhong et al., 2020)(Fig. 8b). However, with the weakening of the NE winds, the influence of the coastal currents diminished, and the warm current expanded. Consequently, nutrient concentrations decreased, and the increasing of abundances of phytoplankton groups with high temperature and salinity niches, such as *Synechococcus*, *Prochlorococcus*, and haptophytes, in the mesotrophic offshore water (Zhong et al., 2020), which was further confirmed by the CCA analysis (Fig. 8).

The distinct phytoplankton community along the cross-front section may have been caused by the formation of the front (Figs 6, 7 and S5, S6). Similar patterns have been reported in the Gerlache Strait, where cryptophytes dominate in the north and abundances of diatoms and *Pyramimonas*-like cells are high in the south (Mascioni et al., 2023), and in the South Brazil Bight, where phytoplankton community dominated by diatoms in the inshore area transitions to a community of nano-sized diatoms and pico-sized flagellates in the outer shelf (Brandini et al., 2018). Studies in the Gerlache Strait (Mascioni et al., 2023; Mendes et al., 2018) have suggested that although the study area is complex, the recurrent spatial patterns of phytoplankton community suggest that responses of phytoplankton community in the TWS to the weakening or strengthening of the NE monsoon may be predictable. Results of PCoA analysis (Fig. 8a) showed that phytoplankton communities in the coastal current were dominated by diatoms, cryptophytes, and dinoflagellates, and they were located on the negative side of the first PCoA axis, especially during the periods of strong NE monsoons. In contrast, the phytoplankton community in the warm current was characterized by high proportions of *Prochlorococcus*, *Synechococcus*, and haptophytes, and was located on the positive side of the first PCoA axis, particularly during the observations when the NE wind was weak (Fig. 8a). The phytoplankton community during the period of moderate NE winds was intermediate between the community associated with the strong NE wind and the community associated with the weak NE wind (Fig. 8a). These results suggested that the positioning of phytoplankton communities in the PCoA analysis was indicative of the intensity of the NE wind. A previous study (Zhong et al., 2022) has reported results of an investigation in March 2016 when the NE wind was relatively strong in the TWS, and at that time the phytoplankton community in the coastal areas of the northern TWS was dominated by diatoms, dinoflagellates, and cryptophytes. The similarity of phytoplankton communities during the observation in 2016 and the periods of strong NE winds further indicated that dynamics of the phytoplankton community may be regulated by the variations of ocean current forcing by the NE winds. During the NE monsoon, the TWS was influenced by the coastal current and the Taiwan warm current, and their intensities underwent obvious variability that was influenced by the changes of the NE winds. Many studies have shown that the satellite SST data agreed with the *in situ* observations in the TWS, and the satellite data pinpointed areas with SSTs $\leqslant 17$℃ that were influenced by coastal currents (Zhang et al., 2020). The results of this study therefore suggested the possibility of rapidly assessing variations of the phytoplankton community based on the dynamics of SST and wind patterns derived from satellite data.

Furthermore, during the NE monsoon, temperature or salinity fronts form in the central TWS when the cold, low-salinity current meets the warm, high-salinity currents (Zhao et al., 2022). The position, width, and intensity of these fronts are largely influenced by monsoonal forces on short timescales (Huang et al., 2015; Pan et al., 2013) and exhibit significant seasonal variations (Hong et al., 2011a). The variations of climatological temperature gradients in the surface water (Fig. 1) from January to May and the different changes of physical variables along cross-front sections during three cruises with different speeds of NE winds further confirmed the influence of monsoonal forces (Figs 1 and 2). Many studies have shown that vertical movements of water in the frontal zones increase the upward transport of nutrients and stimulate increases of phytoplankton biomass (Li et al., 2012; Ruiz et al., 2019; Son et al., 2006; Stukel et al., 2017; Woodson and Litvin, 2015). For instance, Son et al. (2006) and Lv et al. (2022) have observed that spring phytoplankton blooms occur in the coastal front. However, this study revealed a significant decrease of phytoplankton biomass in the surface water within frontal zones during the strong NE monsoon (Figs 2 and S1). This decrease may be attributed to the narrow channel of the TWS itself, which is different from a continental shelf. The effect of the narrow channel combined with the influence of a strong monsoon would enhance the “narrow tube” effect, and resulted in higher wind speeds in the north and south of the TWS (Dang et al., 2022). This further lead to parallel flows of the northward and southward currents and to no exchange of matter and energy at the frontal zones but to significant declines in phytoplankton biomass. Therefore, during the NE monsoon, phytoplankton biomass and community structure on both sides of the front and within the frontal zones are controlled mainly by the dynamics of the ocean currents forced by the intensity of the NE wind.

5 Conclusions

This study has been the first evaluation of the impact of the NE monsoon on the phytoplankton community in the TWS and along several sections across the front formed where the coastal current and the Taiwan warm current meet. The phytoplankton biomass and community began to change in the frontal area, and the community structures within the frontal zones differed on both sides of the front. Despite the inherent complexity and dynamics of the TWS during the NE monsoon, patterns of the phytoplankton composition were regulated by dynamics of ocean currents forced by the speed of the NE wind, and those patterns appeared regularly. During strong NE winds, the coastal current facilitated the formation of a strong front. The phytoplankton community transitioned from inshore groups dominated by diatoms, dinoflagellates, and cryptophytes, to offshore groups with higher proportions of haptophytes Type 8, *Prochlorococcus*, *Synechococcus*, and prasinophytes. As the NE monsoon weakened, concentrations of dinoflagellates and crypto-

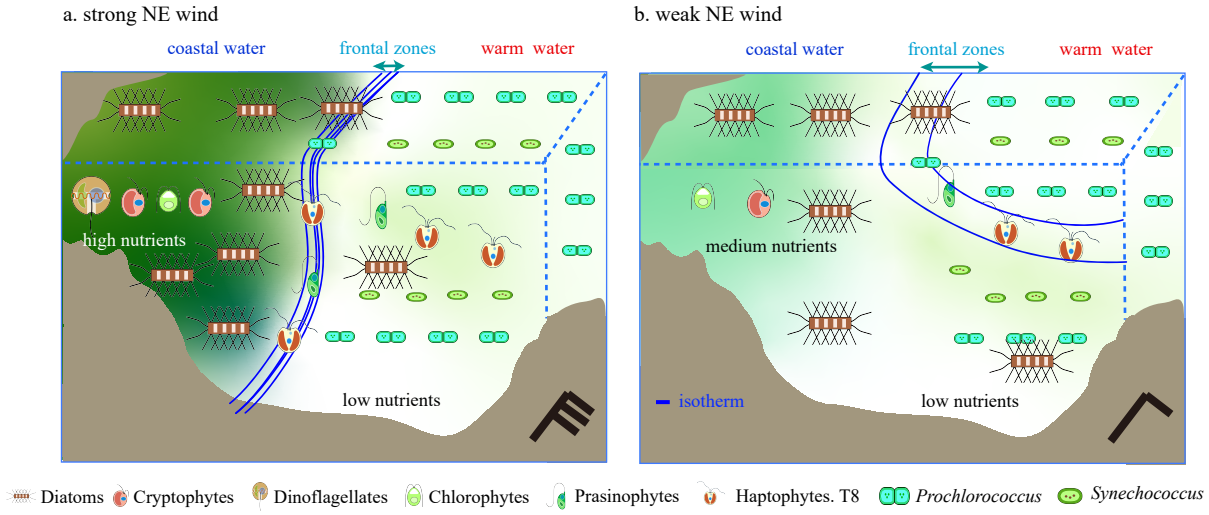

Fig. 9. The ecological responses to the various ocean currents with the weakening of the NE wind in the TWS. a. It represents the ecological responses to the strong NE wind, when the western TWS was influenced by the large influence of the coastal currents; b. it represents the ecological responses to with the weakening of NE wind, when the western TWS was less influenced by the coastal currents.

phytes decreased in the inshore areas, and the concentrations of *Prochlorococcus* and *Synechococcus* increased in the offshore regions (Fig. 9). This study consequently revealed the general response of the phytoplankton community to the different intensities of the NE winds. The influence of the varying NE wind intensities could be rapidly inferred using satellite data on sea surface temperature and wind patterns.

Acknowledgements

Samples were collected onboard the R/V *Yanping 2* during open research cruises NORC2017-04, NORC2018-04, and NORC2019-04 that were supported by the NSFC ship time Sharing Project (project numbers: 41649904, 41749904 and 41849904). We thank Feipeng Xu, Yiyong Jiang, and Lizhen Lin for their assistance in phytoplankton sample collections and analyses, and Liu Siguang for hydrographic data.

References

Belkin I M, Cornillon P C, Sherman K. 2009. Fronts in large marine ecosystems. Progress in Oceanography, 81(1–4): 223–236, doi: 10.1016/j.pocean.2009.04.015

Brandini F P, Tura P M, Santos P P G M. 2018. Ecosystem responses to biogeochemical fronts in the South Brazil Bight. Progress in Oceanography, 164: 52–62, doi: 10.1016/j.pocean.2018.04.012

Chen Yuhan, Lin Heyun. 2022. Overview of the development of offshore wind power generation in China. Sustainable Energy Technologies and Assessments, 53: 102766, doi: 10.1016/j.seta.2022.102766

Clayton S, Nagai T, Follows M J. 2014. Fine scale phytoplankton community structure across the Kuroshio Front. Journal of Plankton Research, 36(4): 1017–1030, doi: 10.1093/plankt/fbu020

Dang Xiaoyan, Bai Yan, Gong Fang, et al. 2022. Different responses of phytoplankton to the ENSO in two upwelling systems of the South China Sea. Estuaries and Coasts, 45(2): 485–500, doi: 10.1007/s12237-021-00987-2

Flint M V, Sukhanova I N, Kopylov I, et al. 2002. Plankton distribution associated with frontal zones in the vicinity of the Pribilof Islands. Deep-Sea Research Part II: Topical Studies in Oceanography, 49(26): 6069–6093, doi: 10.1016/S0967-0645(02)00334-X

He Shuangyan, Huang Daji, Zeng Dingyong. 2016. Double SST fronts observed from MODIS data in the East China Sea off the Zhejiang-Fujian coast, China. Journal of Marine Systems, 154: 93–102, doi: 10.1016/j.jmarsys.2015.02.009

Hong Huasheng, Chai Fei, Zhang Caiyun, et al. 2011a. An overview of physical and biogeochemical processes and ecosystem dynamics in the Taiwan Strait. Continental Shelf Research, 31(6): S3–S12, doi: 10.1016/j.csr.2011.02.002

Hong Huasheng, Liu Xin, Chiang Kuo-Ping, et al. 2011b. The coupling of temporal and spatial variations of chlorophyll *a* concentration and the East Asian monsoons in the southern Taiwan Strait. Continental Shelf Research, 31(6): S37–S47, doi: 10.1016/j.csr.2011.02.004

Hu Jianyu, Kawamura H, Li Chunyan, et al. 2010. Review on current and seawater volume transport through the Taiwan Strait. Journal of Oceanography, 66(5): 591–610, doi: 10.1007/s10872-010-0049-1

Huang Ting-Hsuan, Chen Chen-Tung Arthur, Zhang Wenzhou, et al. 2015. Varying intensity of Kuroshio intrusion into Southeast Taiwan Strait during ENSO events. Continental Shelf Research, 103: 79–87, doi: 10.1016/j.csr.2015.04.021

Kuo Nan-Jung, Ho Chung-Ru. 2004. ENSO effect on the sea surface wind and sea surface temperature in the Taiwan Strait. Geophysical Research Letters, 31(13): L13309, doi: 10.1029/2004GL020303

Lai Chao-Chen, Wu Chau-Ron, Chuang Chia-Ying, et al. 2021. Phytoplankton and bacterial responses to monsoon-driven water masses mixing in the Kuroshio off the east coast of Taiwan. Frontiers in Marine Science, 8: 707807, doi: 10.3389/fmars.2021.707807

Li Qian, Franks P J S, Ohman M D, et al. 2012. Enhanced nitrate fluxes and biological processes at a frontal zone in the southern California current system. Journal of Plankton Research, 34(9): 790–801, doi: 10.1093/plankt/fbs006

Lv Ting, Liu Dongyan, Zhou Peng, et al. 2022. The coastal front modulates the timing and magnitude of spring phytoplankton bloom in the Yellow Sea. Water Research, 220: 118669, doi: 10.1016/j.watres.2022.118669

Mascioni M, Almandoz G O, Cusick A, et al. 2023. Phytoplankton dynamics in nearshore regions of the western Antarctic Peninsula in relation to a variable frontal zone in the Gerlache Strait. Frontiers in Marine Science, 10: 1139293, doi: 10.3389/fmars.2023.1139293

Mendes C R B, Tavano V M, Dotto T S, et al. 2018. New insights on the dominance of cryptophytes in Antarctic coastal waters: a case study in Gerlache Strait. Deep-Sea Research Part II: Topical Studies in Oceanography, 149: 161–170, doi: 10.1016/j.dsr2.2017.02.010

Oziel L, Baudena A, Ardyna M, et al. 2020. Faster Atlantic currents drive poleward expansion of temperate phytoplankton in the Arctic Ocean. Nature Communications, 11(1): 1705, doi: 10.

1038/s41467-020-15485-5
Pan Aijun, Wan Xiaofeng, Guo Xiaogang, et al. 2013. Responses of the Zhe-Min coastal current adjacent to Pingtan Island to the wintertime monsoon relaxation in 2006 and its mechanism. Science China: Earth Sciences, 56(3): 386–396, doi: 10.1007/s11430-012-4429-9
Parab S G, Matondkar S G P, do R. Gomes H, et al. 2006. Monsoon driven changes in phytoplankton populations in the eastern Arabian Sea as revealed by microscopy and HPLC pigment analysis. Continental Shelf Research, 26(20): 2538–2558, doi: 10.1016/j.csr.2006.08.004
R Core Team. 2020. R: A language and environment for statistical computing. Vienna, Austria: R Foundation for Statistical Computing
Ruiz S, Claret M, Pascual A, et al. 2019. Effects of oceanic mesoscale and submesoscale frontal processes on the vertical transport of phytoplankton. Journal of Geophysical Research: Oceans, 124(8): 5999–6014, doi: 10.1029/2019jc015034
Schlitzer R. 2013. Ocean Data View, https://odv.awi.de/
Shang Shaoling, Zhang Caiyun, Hong Huasheng, et al. 2005. Hydrographic and biological changes in the Taiwan Strait during the 1997–1998 El Niño winter. Geophysical Research Letters, 32(11): L11601, doi: 10.1029/2005gl022578
Son S, Yoo S, Noh J H. 2006. Spring phytoplankton bloom in the fronts of the East China Sea. Journal of Ocean Science, 41(3): 181–189, doi: 10.1007/BF03022423
Stukel M R, Aluwihare L I, Barbeau K A, et al. 2017. Mesoscale ocean fronts enhance carbon export due to gravitational sinking and subduction. Proceedings of the National Academy of Sciences of the United States of America, 114(6): 1252–1257, doi: 10.1073/pnas.1609435114
Taylor A G, Goericke R, Landry M R, et al. 2012. Sharp gradients in phytoplankton community structure across a frontal zone in the California Current Ecosystem. Journal of Plankton Research, 34(9): 778–789, doi: 10.1093/plankt/fbs036
Thomson R E, Fine I V. 2003. Estimating mixed layer depth from oceanic profile data. Journal of Atmospheric and Oceanic Technology, 20(2): 319–329, doi: 10.1175/1520-0426(2003)020<0319:EMLDFO>2.0.CO;2
Woodson C B, Litvin S Y. 2015. Ocean fronts drive marine fishery production and biogeochemical cycling. Proceedings of the National Academy of Sciences of the United States of America, 112(6): 1710–1715, doi: 10.1073/pnas.1417143112
Yu Yi, Xing Xiaogang, Liu Hailong, et al. 2019. The variability of chlorophyll-*a* and its relationship with dynamic factors in the basin of the South China Sea. Journal of Marine Systems, 200: 103230, doi: 10.1016/j.jmarsys.2019.103230
Zhang Caiyun, Huang Yan, Ding Wenxiang. 2020. Enhancement of Zhe-Min coastal water in the Taiwan Strait in winter. Journal of Oceanography, 76(3): 197–209, doi: 10.1007/s10872-020-00539-5
Zhao Zhonghua, Oey L Y, Huang Bangqin, et al. 2022. Off-coast phytoplankton bloom in the Taiwan Strait during the northeasterly monsoon wind relaxation period. Journal of Geophysical Research: Oceans, 127(9): e2022JC018752, doi: 10.1029/2022jc018752
Zhong Yanping, Hu Ju, Laws E A, et al. 2019. Plankton community responses to pulsed upwelling events in the southern Taiwan Strait. ICES Journal of Marine Science, 76(7): 2374–2388, doi: 10.1093/icesjms/fsz142
Zhong Yanping, Laws E A, Zhuang Jiafu, et al. 2022. Responses of phytoplankton communities driven by differences of source water intrusions in the El Niño and La Niña events in the Taiwan Strait during the early spring. Frontiers in Marine Science, 9: 997591, doi: 10.3389/fmars.2022.997591
Zhong Yanping, Liu Xin, Xiao Wupeng, et al. 2020. Phytoplankton community patterns in the Taiwan Strait match the characteristics of their realized niches. Progress in Oceanography, 186: 102366, doi: 10.1016/j.pocean.2020.102366

Supplementary information:

Fig. S1. Surface temperature, salinity, and fluorescent chlorophyll based on the Ferrybox system along Transect H during the observations of the strong NE wind (left), Transect E during the observations of the moderate NE wind (middle), and Transect B during the observations of the weak NE wind (right).

Fig. S2. Vertical profiles of sea temperature chlorophy (℃, a, b, c), salinity (d, e, f), potential density anomaly (kg/m^3, g, h, i), buoyancy frequency (cycle/h, j, k, l), and fluorescence chlorophyll (μg/L, m, n, o) along Transects H (a, d, g, j, m), E(b, e, h, k, n), and B (c, f, i, l, o) during the observations with the strong (left), moderate (middle), and weak (right) NE wind.

Fig. S3. Vertical profiles of nitrate + nitrite (NO_X, μmol/L, a, b, c), phosphate (PO_4^{3-}, μmol/L, d, e, f), and silicate (SiO_3^{2-}, μmol/L, g, h, i) along the Transects H, E, and B during the observations with the strong (left), moderate (middle), and weak (right) NE wind.

Fig. S4. Vertical profiles of total chlorophyll *a* (TChl *a*)(ng/L, a, b, c), dinoflagellate (Dino, ng/L, d, e, f), diatoms (Diat, ng/L, g, h, i), cryptophytes (cryp, ng/L, j, k, l), prasinophytes (Pras, ng/L, m, n, o), haptophytes Type 8 (Hapt. T8, ng/L, p, q, r), *Synechococcus* (Syne, ng/L, s, t, u), and *Prochlorococcus* (Proc, ng/L, v, w, x) along the Transects H, E, and B during the observations with the strong (left), moderate (middle), and weak (right) NE wind.

Fig. S5. Phytoplankton compositions in the surface water (upper) and average depth-integrated (bottom) along Transect H during the observations under the forcing of the strong NE wind (left), Transect E during the observations under the forcing of the moderate NE wind (middle), and Transect B under the forcing of the weak NE wind (right). CW: coastal water; FZ: the frontal zone; WW: the warm water.

The supplementary information is available online at https://doi.org/10.1007/s13131-023-2381-0 and http://www.aosocean.com/. The supplementary information is published as submitted, without typesetting or editing. The responsibility for scientific accuracy and content remains entirely with the authors.